

# Approximate Approach to the Design of Shielded Dielectric Disk Resonators with Whispering-Gallery Modes

Eugene N. Ivanov, David G. Blair, and Victor I. Kalinichev

**Abstract**—An analytical method is presented for calculating the resonant frequency and the  $Q$ -factor of shielded dielectric disk resonators excited in whispering-gallery modes. The method is based on a single-mode representation of electromagnetic fields in partial regions of the resonator. For high order modes with high degree of energy concentration in the dielectric this method gives a good agreement with experimental results obtained for different sapphire disks at both room temperature and cryogenic temperatures.

## I. INTRODUCTION

PROPERTIES OF the electromagnetic whispering-gallery modes ( $Wg$ -modes) in a dielectric disk fabricated from a very high purity sapphire crystal mounted inside a cylindrical superconducting cavity has been experimentally investigated by Blair [1]. Extremely high values of the  $Q$ -factor are achievable at these modes (up to  $4.3 \times 10^9$  at  $T = 2.2$  K). The low sensitivity of such resonators to environmental perturbations, along with the presence of turning points in the temperature dependence of resonant frequency [2], [3] allows one to create a very high performance microwave frequency standard with fractional frequency stability less than  $10^{-14}$  for integration time between 3-300 sec [4].

The design of such resonators requires the accurate computation of the resonant frequency and the  $Q$ -factor of the operating mode. Although there are a number of rigorous and approximate approaches to analysis of Shielded Dielectric Disk Resonators (SDR), these are generally devoted to low-order modes in miniature ceramic resonators of very high permittivity  $\epsilon > 30$  [5]. The method described here is an extension of an approximate one which has been used previously for analysis of high-order modes in open sapphire disk resonators [6]. It belongs to the group of mode matching methods and is a simplified version of the Partial Region Method (PRM) [7]. According to this method electromagnetic fields in the each partial region of the cavity are expressed in terms of single eigenmodes with unknown amplitude coefficients. The coefficients are found by the process of matching tangential components of the  $H$  and  $E$  fields on the boundary between

Manuscript received March 25, 1992; revised July 30, 1992. This research was supported in part by the Australian Research Council.

E. N. Ivanov and D. G. Blair are with the Physics Department, University of Western Australia, Nedlands, Australia, 6009.

V. I. Kalinichev is with the Moscow Power Engineering Institute, Moscow, Russia.

IEEE Log Number 9206307.

adjacent regions. This matching also results in a system of characteristic equations which allows the resonant frequency to be defined.

As for the fundamental  $Wg$ -modes in the open sapphire cavity the accuracy of the frequency calculation using this method improves with the growth of azimuth number  $m$  and can be about 0.1% for  $m > 6-8$  [6]. This is because most of the electromagnetic energy of  $Wg$ -mode is confined to a small region near the circumference of the disk and one can neglect the scattered fields near the disk edges. For low-order  $Wg$ -modes ( $m < 6$ ) in comparatively “thin” disks, this assumption is not exactly true and more rigorous modifications of the PRM must be used.

In this paper we first consider a simple 2 dimensional model for SDR's, which is useful for understanding their general properties. In Section III we describe the generalized 3 dimensional model. Results of computation and comparison with experiment are presented in Section IV, while in Section V we discuss the limits of our mathematical model.

## II. PROPERTIES OF $Wg$ -MODES IN INFINITE SDR

A schematic drawing of the SDR is shown in Fig. 1. To qualitatively explain some basic properties of the SDR it is enough to consider a two-dimensional model consisting of an infinite dielectric rod placed coaxially inside a cylindrical metal shield. Such a model allows one to study the influence of shield on the  $Q$ -factor of  $Wg$ -modes, and to understand why the total sizes of the SDR can be much smaller than those of an open unshielded resonator.

The general solution of this problem for waves travelling along the  $\varphi$ -direction has been obtained in [8]. We use some of these results to study in detail one of the most important situations: a sapphire rod inside a copper shield. Calculations have been accomplished for two mode families existing independently in the SDR under such conditions: for  $E$ -modes characterized by  $E_z, H_\rho, H_\varphi$ -components and for  $H$ -modes with  $H_z, E_\rho, E_\varphi$ -components. The frequency dependence of the sapphire loss tangent and the surface resistivity of copper at room temperature are assumed to be described by the following empirical equations:  $\tan \delta = 5 \times 10^{-7} f$ , where  $f$  is a frequency in GHz, and  $R_s = 4.45 \times 10^{-3} \sqrt{f/V_c}$ , where  $f$  is a frequency in Hz and  $V_c$  is the velocity of the light in vacuum in m/sec. The radius of the sapphire rod  $b$  is assumed to be kept constant whereas the

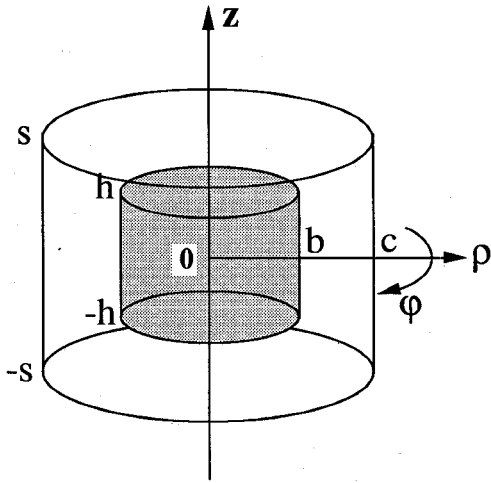


Fig. 1. Schematic drawing of the shielded dielectric disk resonator.

shield radius  $c$  is varied from  $c = b$  to  $c = 5b$ . The value  $b$  chosen, 17.2 mm, is a typical value for  $X$ -band cavities.

Results of calculations for fundamental  $E$ - and  $H$ -modes with one node along the radius and  $m$  nodes in the azimuthal direction are shown in Fig. 2(a) and (b), respectively. The mechanism of the maximums in Fig. 2(a) and (b) is related to non-monotonic dependence of the power losses in the metal shield at variations of its radius. The maximum value of  $Q$  for  $E$ -modes is achieved at smaller azimuthal number ( $m = 4$ ) than for  $H$ -modes ( $m = 6$ ). This property which holds also for three dimensional SDR can be used to substantially reduce the size and cost of dielectric disk resonators. For instance, at  $f = 10$  GHz the radius of the dielectric rod is equal to 8.8 mm for  $E_{4,1}$ -mode and 15.1 mm for  $H_{6,1}$ -mode. In both cases the  $Q$ -factor is dominated by only the intrinsic losses in sapphire ( $Q = 2 \times 10^5$ ) provided the shield radius is chosen to be equal to 23–25 mm.

Such  $Q$ -factors are unachievable in open resonant systems, (such as a solid dielectric rods or disks in free space) if low azimuth numbers ( $m = 4$ –6) because large radiation losses. Thus the  $Q$ -factor of  $E_{4,1}$ -mode in an open resonator does not exceed  $10^3$  [9]. To make the radiation losses negligible compared with the power dissipated in the dielectric it is necessary to increase the azimuth number and simultaneously the radius of the rod in order to keep the resonant frequency constant. From our previous work [9] one can calculate that radiation losses cease to restrict the  $Q$ -factor of the  $E$ -modes for  $m > 9$ . In this case the sapphire rod radius must be 17 mm to allow a 10 GHz resonant frequency.

Therefore, at least two main advantages of SDR become evident from the two-dimensional model: small sizes, and associated with them, a less dense spectrum of resonant mode frequencies. It is also worth emphasizing here one principal feature of SDRs revealed by the  $Q$ -value computations. The maximum value of the SDR  $Q$ -factor can exceed the level determined by intrinsic losses in the dielectric. For  $Wg$ -modes with  $m = 5$ –8 the excess is about a few percent.

Another results obtained from the two-dimensional model concern the dependence of resonant frequency on geometry. In particular, Fig. 3 shows the free space wave number  $k =$

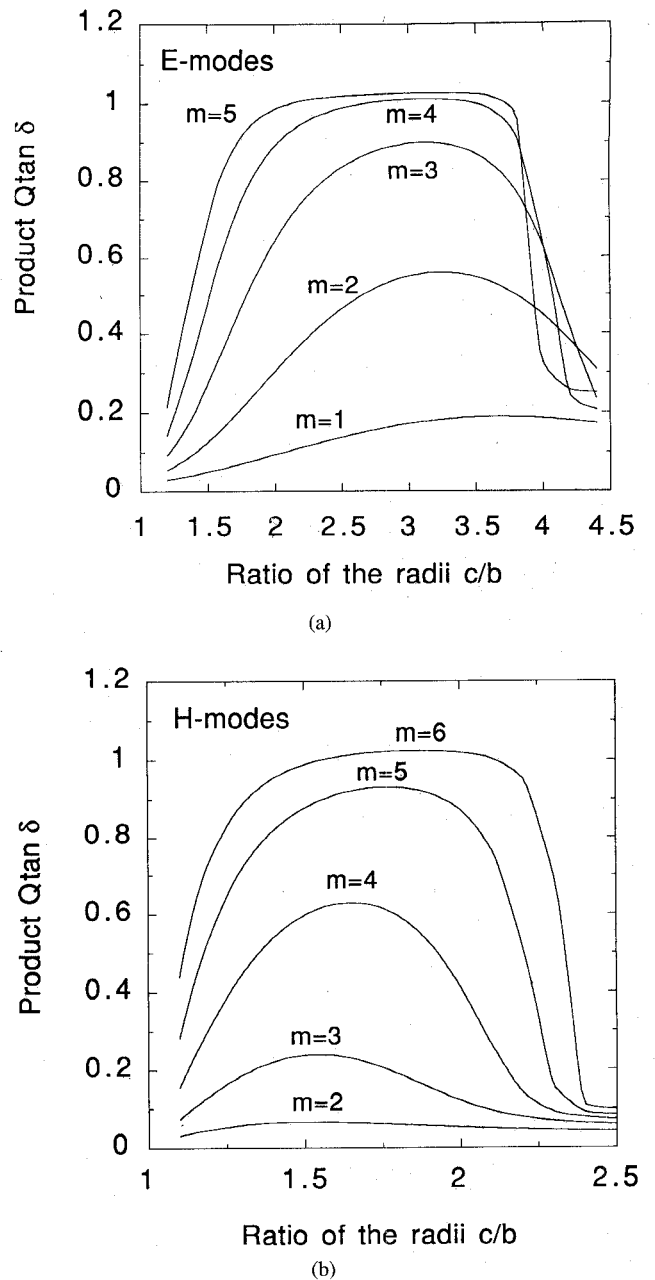


Fig. 2.  $Q$ -factor as a function of the ratio of the shield radius to dielectric rod radius for  $E$ -modes and  $H$ -modes at room temperature. (a)  $E$ -modes. (b)  $H$ -modes.

$2\pi f/V_c$  as a function of the ratio of the shield radius  $c$  to the rod radius  $b$  for two modes  $E_{8,1}$  and  $H_{8,1}$ . The different behavior of the resonant frequencies of  $E$ - and  $H$ -modes at variations of the shield radius allows a simple way of mode identification in the real three dimensional SDR.

### III. GENERAL EQUATIONS AND ITS SOLUTION

In accordance with the partial region approach, the expressions for the  $z$ -components of the electromagnetic field in different regions of the SDR can be presented in the same manner as was done in [6]. By matching tangential components of the  $H$  and  $E$  fields on the cylindrical surface of the dielectric disk ( $\rho = b$ ) and requiring the vanishing of  $E_z$  and

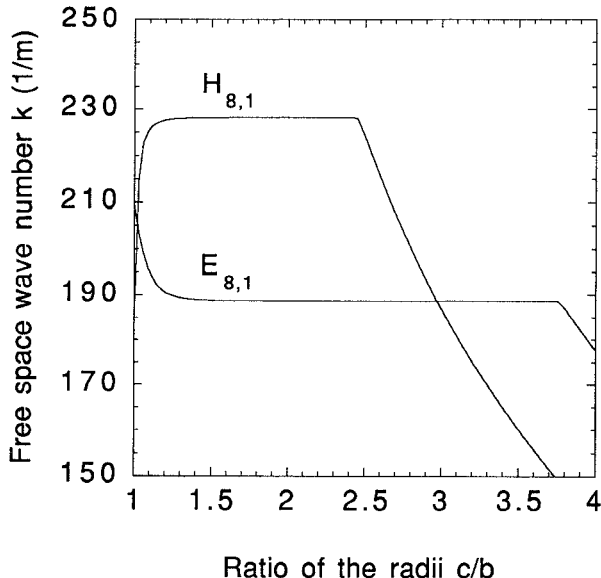


Fig. 3. Resonant frequencies of  $H_{8,1}$ - and  $E_{8,1}$ -modes of the shielded dielectric rod resonator versus ratio of the shield radius to dielectric rod radius.

$E_\varphi$  at the surface of metal side walls ( $\rho = c$ ) we can obtain the following characteristic equation:

$$\begin{aligned} & \left[ \frac{\epsilon_n g_\tau g_e}{g_n^2} J_m(g_\tau b) - \frac{f_3}{f_2} J_m(g_\tau b) \right] \\ & \cdot \left[ \frac{g_3}{g_n} J_m(g_n b) - \frac{f_1}{f_4} J_m(g_n b) \right] g_3^2 \\ & = J_m(g_\tau b) J_m(g_n b) \left[ \frac{m\beta}{kb} \right]^2 \left[ \frac{g_3^2 - g_n^2}{g_n^2} \right]^2, \end{aligned} \quad (1)$$

where

$$f_1 = J_m(g_3 b) \dot{Y}_m(g_3 c) - \dot{J}_m(g_3 c) Y_m(g_3 b) \quad (2.1)$$

$$f_2 = J_m(g_3 b) Y_m(g_3 c) - J_m(g_3 c) Y_m(g_3 b), \quad (2.2)$$

$$f_3 = \dot{J}_m(g_3 b) Y_m(g_3 c) - J_m(g_3 c) \dot{Y}_m(g_3 b), \quad (2.3)$$

$$f_4 = J_m(g_3 b) \dot{Y}_m(g_3 c) - \dot{J}_m(g_3 c) Y_m(g_3 b). \quad (2.4)$$

Here  $J_m$  and  $Y_m$  are Bessel and Neumann functions of the order  $m$ , respectively. The dot over  $J_m, Y_m$  denote derivatives with respect to the argument. Equation (1) relates two unknown values: the free space wave number  $k$  and the longitudinal propagation constant  $\beta$ . All other parameters in (1) can be expressed through  $k$  and  $\beta$ :  $g_3^2 = k^2 - \beta^2$ ,  $g_n^2 = k^2 \epsilon_n - \beta^2$ ,  $g_\tau^2 = (\epsilon_\tau / \epsilon_n) g_n^2$ , where  $\epsilon_\tau$  and  $\epsilon_n$  are components of permittivity tensor parallel and perpendicular to  $z$ -axis of the disk. Crystal axis of sapphire is supposed to be parallel to symmetry axis of resonator.

Characteristic equation (1) is valid only for  $k > \beta$ . For  $k < \beta$  (1) becomes

$$\begin{aligned} & \left[ \frac{\epsilon_n g_\tau h_3}{g_n^2} \dot{J}_m(g_\tau b) + \frac{\varphi_3}{\varphi_2} J_m(g_\tau b) \right] \\ & \cdot \left[ \frac{h_3}{g_n} \dot{J}_m(g_n b) + \frac{\varphi_1}{\varphi_4} J_m(g_n b) \right] h_3^2 \\ & = J_m(g_\tau b) J_m(g_n b) \left[ \frac{m\beta}{kb} \right]^2 \left[ \frac{h_3^2 + g_n^2}{g_n^2} \right]^2, \end{aligned} \quad (3)$$

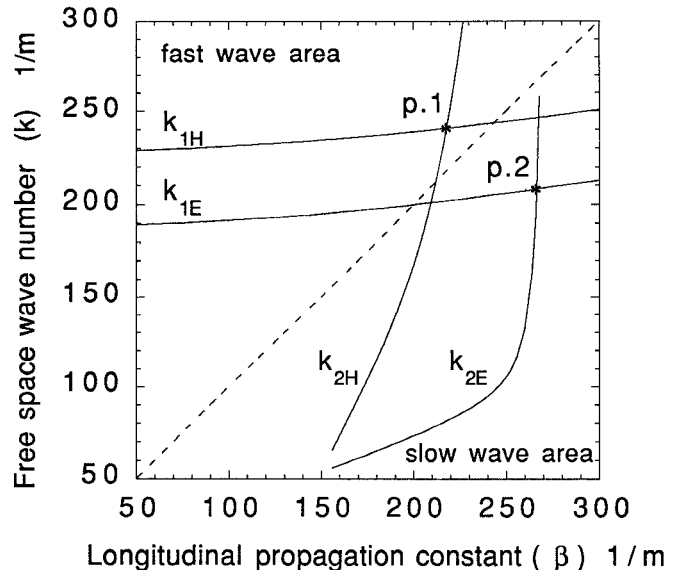


Fig. 4. Graphical solution of the system of characteristic equations for  $m = 8, b = 17.2$  mm,  $2h = 11.5$  mm,  $c/b = 1.6$  and  $s/h = 2$ .

where  $h_3^2 = \beta^2 - k^2$ . The expressions for  $\varphi_1 \dots \varphi_4$  are obtained from the corresponding expressions for  $f_1 \dots f_4$  by changing the Bessel functions  $J_m, Y_m$  to modified ones  $I_m, K_m$ . For example,

$$\varphi_1 = \dot{I}_m(h_3 b) \dot{K}_m(h_3 c) - \dot{I}_m(h_3 c) \dot{K}_m(h_3 b).$$

At a given value of  $\beta$  (1) represents an oscillating function of  $k$  with the infinite number of roots. The dependencies of the first two smallest roots,  $k_{1E}$  and  $k_{1H}$ , versus  $\beta$ , obtained at  $m = 8, b = 17.2$  mm,  $c/b = 1.6$  are shown in Fig. 4. These dependencies describe the behaviour of hybrid electromagnetic waves with one field variation along the radius and  $m$  variations along azimuthal direction, propagating in a shielded dielectric rod waveguide. Subscripts  $E$  and  $H$  imply that in the limiting case when  $\beta = 0$ , hybrid modes characterized by  $k_{1E}$  and  $k_{1H}$  wave numbers are transformed into the  $E$ - and  $H$ -modes, respectively, of the infinite SDR. For  $k > \beta$  (i.e., in the field above the  $k = \beta$  line in Fig. 4) the phase velocity of hybrid waves  $V_{ph}$  is larger than velocity of light  $V_c$ , while for  $k < \beta$  we have  $V_{ph} < V_c$ .

In order to study the solution of (1) or (3) in the transition region where  $V_{ph} = V_c$ , both analytical and numerical approaches can be used. The former requires the use of expansions for cylindrical functions  $J_m(x)$  and  $Y_m(x)$  as  $x \rightarrow 0$  and results in a very cumbersome equation with respect to  $k$ . We employ the latter approach, and linearly interpolate the real curve  $k(\beta)$  in the small region about the point  $k = \beta$ . This is a more universal method to find the general solution at  $k = \beta$  as it may be used for analysis of other similar structures, such as the shielded dielectric ring resonator.

Another set of characteristic equations complementary to (1) follows from the boundary conditions on the top of the disk ( $z = h$ ) and on the surface of the metal lid ( $z = s$ ). To get these equations in the framework of present model we must

assume that one of the two longitudinal field components of hybrid mode becomes zero in the process of axial matching. Assuming this, for the transverse magnetic or  $E$ -mode, with a symmetrical field distribution inside the disk ( $E_z \sim \cos \beta_z$ ) we obtain the following characteristic equation

$$\beta \tan\{\beta h\} = \varepsilon_n \alpha \tanh\{\alpha(s - h)\}, \quad (5)$$

where  $\alpha^2 = k^2(\varepsilon_r - 1) - \beta^2(\varepsilon_r/\varepsilon_n)$ ,  $h$  is a half height of the dielectric disk and  $s$  is a half height of the metal cavity.

A similar equation for the transverse electric or  $H$ -mode, with  $H_z \sim \cos \beta_z$ , is given by

$$\beta \tan\{\beta h\} = \alpha / \tanh\{\alpha(s - h)\}, \quad (6)$$

where

$$\alpha^2 = k^2(\varepsilon_n - 1) - \beta^2.$$

In the latter case it is necessary to bear in mind that for  $\beta < \beta_{cr}$ , where  $\beta_{cr}$  is the root of the equation  $\beta \tan\{\beta h\} = 1/(s - h)$ , (6) has to be rewritten as

$$\beta \tan\{\beta h\} = \alpha / \tan\{\alpha(s - h)\}, \quad (7)$$

where  $\alpha^2 = \beta^2 - k^2(\varepsilon_n - 1)$ . The physical reason for this is that the resonant frequency of  $H$ -modes increases when the clearance  $t = s - h$  between the dielectric and the metal surfaces decreases, and above a certain critical value of  $t$  (when  $\beta < \beta_{cr}$ ) the resonant frequency becomes larger than the cutoff frequency of hollow waveguide above the dielectric disk. For  $E$ -modes such a problem does not arise as their resonant frequency reduces with decreasing  $t$ .

Equations (5) and (6) do not permit an analytical solution, so that the function  $k(\beta)$  must be obtained numerically. The form of  $k(\beta)$ , denoted  $k_{2E}$  and  $k_{2H}$  for  $E$ - and  $H$ -modes, respectively, are shown in Fig. 4. These results were obtained at  $2h = 11.5$  mm,  $s/h = 2$  and  $\beta < \beta_{max} = \pi/2h$ , i.e., for modes with one field variation along  $z$ -axis.

The graphical solution of the system of characteristic equations (1)–(6) is determined by the intersection points p.1 and p.2 in Fig. 4. For the specified geometry of the SDR, the resonant frequency of the hybrid  $H_{8,1,1}$ -mode (p.1) is larger than that of hybrid  $E_{8,1,1}$ -mode (p.2). However, point p.2 moves to the right along the curve  $k_{1E}$  faster than point p.1 along  $k_{1H}$  when the height of the disk is decreased. This results in the resonant frequency of hybrid  $E$ -mode in the disk with large  $b/2h$  ratio being larger than that of hybrid  $H$ -mode.

Fig. 4 also shows that the operating regime of SDRs may be quite different depending on the type of mode. Thus, for the  $E_{8,1,1}$ -mode (where the solution is in the fast phase velocity area) the electromagnetic fields in the region outside the dielectric disk are described by oscillating functions  $J_m(x)$  and  $Y_m(x)$ . In contrast, for the  $H_{8,1,1}$ -mode, the radial dependence of external fields is a superposition of exponentially varying functions  $I_m(x)$  and  $K_m(x)$ .

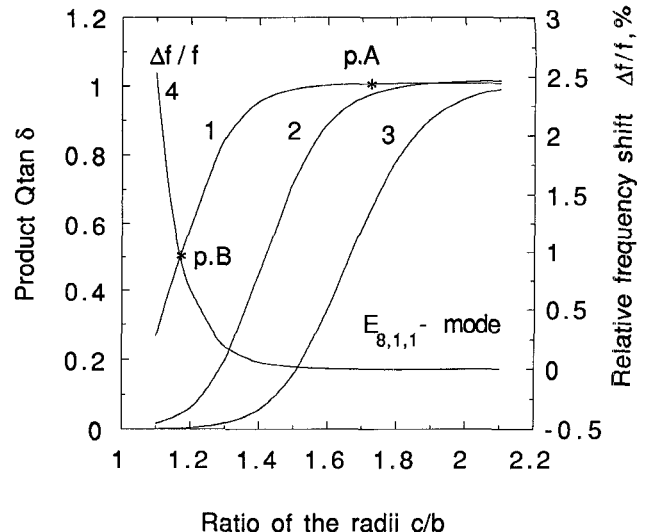


Fig. 5. Product  $Q \tan \delta$  (curves 1, 2, 3) and relative frequency shift (curve 4) as a function of the ratio of the shield radius to dielectric disk radius for  $E_{8,1,1}$ -mode and sapphire disk sizes  $b = 2h = 17.2$  mm. Curve 1:  $s/h = 1.2, T = 293$  K, copper shield. Curve 2:  $s/h = 2.5, T = 4.2$  K, niobium shield. Curve 3:  $s/h = 2.5, T = 4.2$  K, copper shield.

#### IV. DISCUSSION

In the following section the resonant frequency obtained from the numerical solution of (1)–(6) is used to compute the modal field distribution in the SDR and its  $Q$ -factor. During this process all six field components of hybrid mode are taken into account except the partial region above the dielectric disk. Here, as mentioned above, field components  $E_z$  and  $H_z$  can not coexist and one of them must be set equal to zero.

Fig. 5 shows the influence of the metal shield radius on the  $Q$ -factor and the resonant frequency of a mode for a dielectric disk with  $b = 2h = 17.2$  mm. The curves designated by numbers 1, 2, 3 in Figs. 5 and 6 characterize three important practical cases: {1} a room temperature SDR with copper shield, {2} a liquid He-temperature SDR with a niobium shield and {3} a liquid He-temperature SDR with copper shield. For all curves in the Fig. 5 the height of the metal cavity  $s$  is large enough and does not restrict the  $Q$ -factor.

The results at liquid He-temperature were obtained for  $\tan \delta = 2.4 \times 10^{-10}$  [3] and the temperature dependence of the surface resistivity of niobium  $R_s$  given by the following equation [10]:

$$R_s, \text{ ohm} = B \omega^{1.7} \cdot \exp \left[ -1.88 \frac{T_c}{T} \Delta(T) \right] + R_{\text{res}}, \quad (8)$$

where  $B = 7.1 \times 10^{-22}$ ,  $\omega$  is the angular resonant frequency in rad/sec,  $T_c = 9.25$  K,

$$\Delta(T) = \sqrt{\cos \frac{\pi}{2} \left( \frac{T}{T_c} \right)^2}, R_{\text{res}} = 5 \times 10^{-8} \text{ ohm}.$$

For copper we considered that  $R_s(4.2 \text{ K}) = R_s(293 \text{ K})/50$ . Curve 4 in Fig. 5 gives the relative frequency shift  $\Delta f/f$

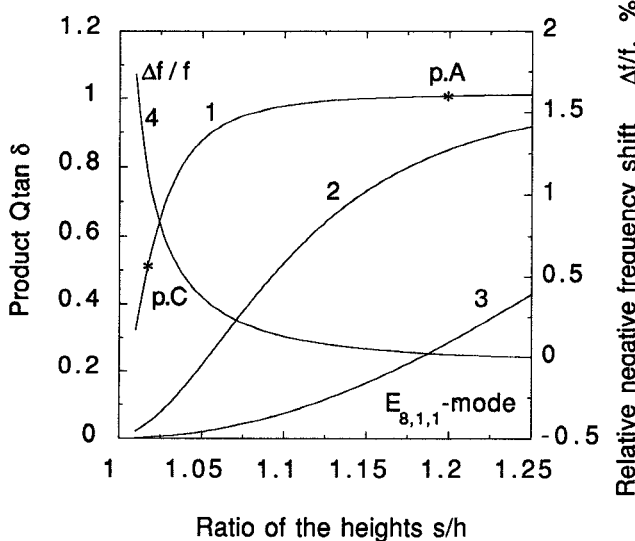


Fig. 6. Product  $Q \tan \delta$  (curves 1, 2, 3) and relative negative frequency shift (curve 4) as a function of the ratio of the metal cavity height to dielectric disk height for  $E_{8,1,1}$ -mode and sapphire disk sizes  $b = 2h = 17.2$  mm. Curve 1:  $c/b = 1.7$ ,  $T = 293$  K, copper shield. Curve 2:  $c/b = 1.9$ ,  $T = 4.2$  K, niobium shield. Curve 3:  $c/b = 2.2$ ,  $T = 4.2$  K, copper shield.

as a function of the shield radius. Like the resonant frequency of  $E$ -mode in the two-dimensional model (Fig. 3) the resonant frequency of hybrid  $E$ -mode goes up when the shield radius decreases.

The  $Q$ -factor and frequency shift as a function of the metal cavity height are shown in Fig. 6. Unlike the previous case, the frequency shift here is negative and increases rapidly with decreasing the height of the metal cavity. This means that under certain conditions the resonant frequency of the SDR can be made independent of the position of the metal walls and its surface reactance. Hence, the temperature dependence of the SDR resonant frequency will be determined by only the temperature dependent dielectric constants  $\epsilon_r$  and  $\epsilon_n$ .

To understand the dependence of SDR properties on geometry it is useful to examine relative power losses and stored energy in different regions of the SDR. The results are given in Table I. Thus, when the metal cavity radius decreases from  $c = 1.7b$  to  $c = 1.2b$  (transition from p.A to p.B in Fig. 5), the SDR  $Q$ -factor decreases by about a factor of two due to the growth losses in the side walls (see Table I). The distribution of the stored energy in SDR in this case varies only slightly. On the other hand, when the height of the metal cavity decreases (transition from p.A to p.C in Fig. 6) the decrease of the  $Q$ -factor arises as a result of big power losses in the end lids (see Table I). It should be noted that the losses in the end lids of the SDR decrease faster than in the side walls which causes the difference in the rising curves in Figs. 5 and 6. The physical reason for this is the more fast decay of the external (with respect to the sapphire disk) electromagnetic fields in the axial direction than in the radial one.

The above model has been applied to the first Sapphire Loaded Superconducting Cavity (SLOSC). The sapphire resonator was a 31.8 mm diameter cylinder, 30.2 mm length, with integral (thin) mounting spindles at each end and the crystal  $c$ -axis coinciding within 1 degree of the geometrical axis. The

TABLE I

		p.A	p.B	p.C
Relative power losses	in the dielectric disk	0.9891	0.4805	0.4815
	in the side walls	0.0024	0.5156	0.0014
	in the end lids	0.0084	0.0038	0.517
Relative energy stored	in the dielectric disk	0.9823	0.9880	0.9605
	between two cylindr. surfaces	0.0044	0.0043	0.0259
	in the space above and under disk	0.0132	0.0077	0.0135

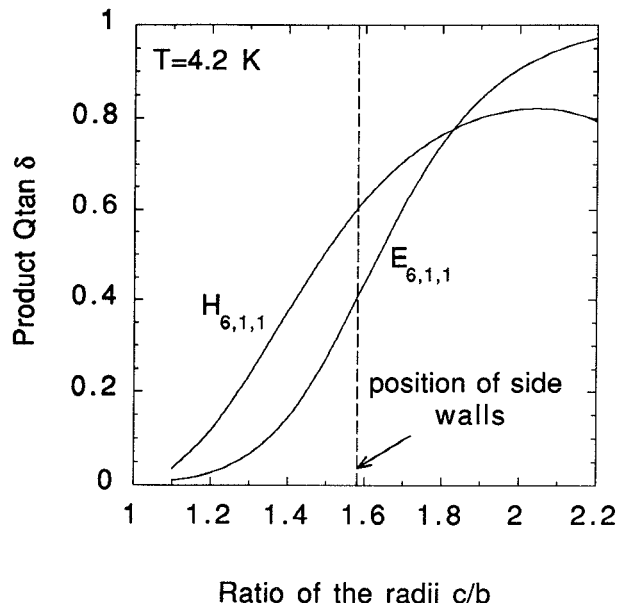


Fig. 7. Product  $Q \tan \delta$  as a function of the ratio of the radii  $c/b$  for  $H_{6,1,1}$ - and  $E_{6,1,1}$ -modes in the SLOSC.

sapphire was mounted in a cylindrical niobium cavity with radius 50 mm and height 50 mm.

For fundamental modes with  $m = 6-10$  the difference between the calculated and measured frequencies is approximately 0.06-0.1% for the same values of  $\epsilon_n$  and  $\epsilon_r$  (9.289 and 11.355 at  $T = 4.2$  K, respectively), which were used in [6].

The  $Q$ -factor computed for two modes  $H_{6,1,1}$  and  $E_{6,1,1}$  is shown in Figs. 7 and 8. First of these modes with  $f_{\text{res}} = 9.73$  GHz and  $Q = 2 \times 10^9$  at  $T = 4.2$  K was the operating one in the SLOSC [4]. From the results presented in Figs. 7 and 8 we can conclude that despite of the very large measured quality factor its value is about 60% of the maximum achievable level. Two main reasons restrict the SLOSC  $Q$  at  $T = 4.2$  K: small azimuth number and power losses in the side walls. The  $Q$ -factor at the given operating frequency could be increased by increasing the size of the shield. Another way to increase the  $Q$ -factor without changing the cavity design is to cool the resonator below 4 K. We estimate that at  $T = 2.2$  K the power losses in the side walls will be much smaller than power dissipation in the dielectric which is practically

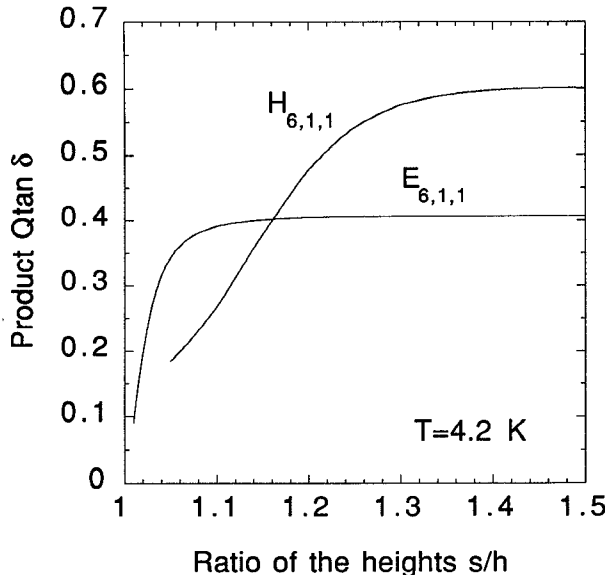


Fig. 8. Product  $Q \tan \delta$  as a function of the ratio of the heights  $s/h$  for  $H_{6,1,1}$ - and  $E_{6,1,1}$ -modes in the SLOSC.

independent on the temperature for  $T < 8$  K [11], and the SLOSC  $Q$ -factor will reach its maximum value. Theoretical and experimental dependence of the  $Q$ -factor on temperature for the above SLOSC are shown in Fig. 9. They demonstrate a good agreement in the temperature range 2–6 K.

##### V. RESTRICTIONS OF THE MODEL

The assumptions made during the deduction of characteristic equations (1)–(6) and expressions for the  $Q$ -factor restrict the accuracy of the model. To test the limits of validity of the model, the height of the sapphire disk was allowed to approach to infinity and the results were compared with the ones obtained from the two-dimensional model. It was found that for  $E$ -modes with  $m < 5$  the three-dimensional model does not describe adequately the  $Q$ -factor when the shield radius  $c$  is big enough. For example, at  $m = 5$  the maximum shield radius  $c_{\max}$  must be lower than  $2.6b$ . It should be noted that in this case the model is formally valid, because a hollow waveguide of radius  $c$  remains below cutoff, while  $c < 3.95b$ .

For  $H$ -modes the results of three-dimensional modelling converge well to the exact solution even at  $m = 4$  for shield radii varying in the whole operating range from  $c = b$  to  $c = 2.3b$ .

For our model to be consistent with experiment, the minimum value of the azimuth number must be equal to 6 and the  $b/2h$  ratio must not exceed 1.5–2.

##### VI. CONCLUSION

A simple version of the Partial Region Method has been applied to the analysis of whispering-gallery modes in shielded dielectric disk resonators. For modes with high azimuth numbers ( $m > 6$ ) the method presented allows a detailed design of such resonators including the optimization of their geometry, quality factors and susceptibility to shield vibrations. During the work on this paper this method has been successfully

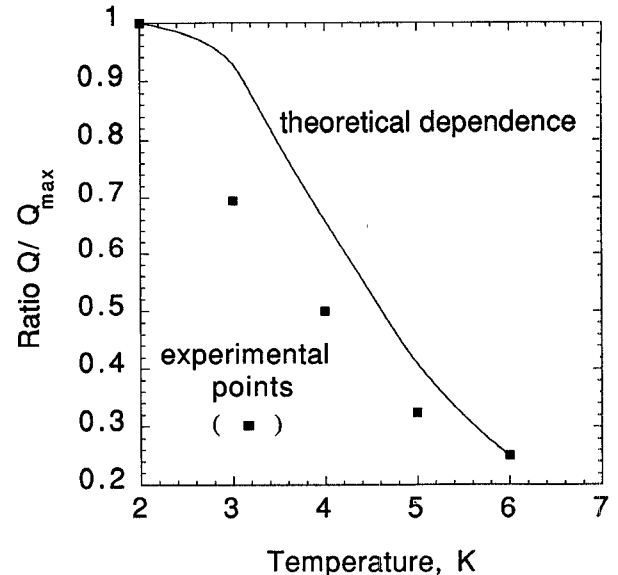


Fig. 9. Normalized value of the  $Q$ -factor versus temperature for  $H_{6,1,1}$ -mode in the SLOSC. Calculated results are represented by continuous line, experimental data by black squares.

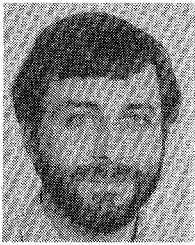
used in order to design the room temperature SDR's with the smallest possible sizes and the  $Q$ -factor dominated by the only intrinsic losses in sapphire. Such cavities allow a very low density of spurious modes and can have valuable applications in the microwave techniques.

##### ACKNOWLEDGMENT

The authors wish to thank Dr. Anthony Mann and Dr. Marco Costa for their general assistance and valuable advice.

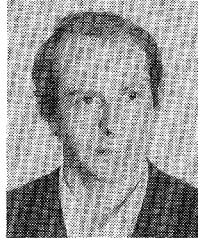
##### REFERENCES

- [1] D. G. Blair and S. K. Jones, "A high- $Q$  sapphire loaded superconducting cavity resonator," *J. Phys. D: Appl. Phys.*, vol. 20, pp. 1559–1566, 1987.
- [2] S. K. Jones, D. G. Blair, and M. J. Buckingham, "Effect of paramagnetic impurities on frequency of sapphire loaded superconducting cavity resonators," *Electron. Lett.*, vol. 24, no. 6, pp. 364–347, 1988.
- [3] S. K. Jones and D. G. Blair, "High-quality factors for a sapphire-loaded superconducting cavity resonator," *Electron. Lett.*, vol. 23, no. 16, pp. 817–818, 1988.
- [4] A. J. Giles, S. K. Jones, D. G. Blair, and M. J. Buckingham, "A high stability oscillator based on a sapphire-loaded superconducting cavity," *Proc. 43rd Ann. Freq. Control Symp.*, 1989, pp. 89–93.
- [5] M. Tsuji, H. Shigesawa, and K. Takiyama, "On the complex resonant frequency of open dielectric resonators," *IEEE Trans. Microwave Theory Tech.*, vol. 31, no. 5, pp. 392–396, 1988.
- [6] M. Tobar and A. Mann, "Resonant frequencies of higher order modes in cylindrical anisotropic dielectric resonators," *IEEE Trans. Microwave Theory Tech.*, vol. 39, no. 12, pp. 2077–2082.
- [7] D. Kajfez and P. Guillon, *Dielectric Resonators*. Norwood, MA: Artech House, 1988.
- [8] V. F. Vzyatyshev, V. I. Kalinichev, and V. I. Kuimov, "Physical phenomena in shielded dielectric rod resonator and problems of its design," *Radio Engineering and Electronic Physics*, no. 4, pp. 705–712, 1985.
- [9] E. N. Ivanov and V. I. Kalinichev, "Analysis of complex spectrum of open dielectric resonator," *Radiotekhnika*, no. 2, pp. 40–42, 1988.
- [10] V. B. Braginsky, V. P. Mitrofanov, and V. I. Panov, *System with Small Dissipation*. Chicago: University of Chicago Press, 1985.
- [11] V. B. Braginsky, V. S. Ilchenko, and K. S. Bagdassarov, "Experimental observation of fundamental microwave absorption in high-quality dielectric crystals," *Physics Letters A*, vol. 120, no. 6, pp. 300–305, 1987.



**Eugene N. Ivanov** was born in Moscow, Russia, on August 14, 1956. He received the "Diploma of Engineer" in radio engineering in 1979 and the Ph.D. degree in radio electronic systems in 1987, both from Moscow Power Engineering Institute (MPEI). His dissertation was entitled "Low-phase-noise Gunn oscillators with electronic tuning of operating frequency."

From 1979 to 1991 working at the Department of Radio engineering of MPEI (except the period 1982-84 when he served in the anti-aircraft unit) he was engaged in the development of low-noise microwave oscillators for radar and communication systems. In 1980 in common with Dr. D. Tsarapkin he employed a new type of microwave resonators—sapphire dielectric disk resonator excited in whispering-gallery modes—for frequency stabilization of Gunn diode oscillator. His research interests include frequency stabilization of microwave oscillators, noise phenomena in microwave systems and applied electrodynamics. In 1990 in collaboration with Dr. V. Kalinichev he developed a concept of sapphire loaded circuits with enhanced  $Q$ -factor and studied its performance. Since 1991 he has been with the University of Western Australia as a Research Associate on the Sapphire Clock Project and Gravity Wave Project. He is currently involved in the design of microwave signal processing system for gravitational wave antenna with non-contacting readout.



**Victor I. Kalinichev** graduated from the Radio Engineering Faculty of the Moscow Power Engineering Institute (MPEI) in 1977. He received the Ph.D. degree in radiophysics and electronics from the MPEI in 1984.

Since 1983 he has been with the Radio Engineering Department of the MPEI and has been engaged in the research and development of microwave/millimeter wave passive structures and integrated circuits based on dielectric waveguides. His current professional interests include modeling and

design of various millimeter wave circuits, components, and devices.



**David G. Blair** was born in Hampshire, England, on November 25, 1946. He received the B.Sc.(hons) degree in physics from the University of Western Australia in 1967. In 1972 he received the Ph.D. degree from the University of East Anglia, England. His dissertation was entitled "Superflow: A Study of Superfluid Helium Films."

From 1972 to 1973 he was a Science Research Associate at the University of East Anglia. His research included design of high-vacuum, optical, cryogenic, and superconducting apparatus. From 1973 to 1976 he was a Visiting Assistant Professor at Louisiana State University. Since 1976 he has been with the University of Western Australia, where he is now an Associate Professor in the Department of Physics. He is a chief investigator and initiator of the Gravitational Radiation Research Project at the University of Western Australia. His research has included the study of low acoustic loss systems, high  $Q$  electromagnetic resonators, design of gravitational wave detectors, the birthrate of supernovae and pulsars as sources of gravitational waves.